Nuclear Magnetic Resonance in Ferrimagnetic $MnFe_2O_4$

A. J. HEEGER* AND T. W. HOUSTON
Laboratory for Research on the Structure of Matter†
Department of Physics, University of Pennsylvania, Philadelphia, Pennsylvania
(Received 10 March 1964)

The Mn^{55} nuclear magnetic resonance has been studied in $MnFe_2O_4$. The unpulled resonance frequency extrapolated to 0°K is 587 Mc/sec. By studying the effect of an external magnetic field on the resonance it was determined that the main line at low temperatures arises from nuclei within the bulk of the single domains; and that the hyperfine coupling constant A is negative. The form of the single-domain enhancement factor was verified. At higher temperatures, the signal comes from nuclei within the domain walls. Frequency pulling effects associated with both the wall nuclei and bulk nuclei are observed in the liquid-helium temperature range. The temperature dependence of the Mn^{55} frequency was used to study the temperature dependence of the A-site sublattice magnetization. The results are in excellent agreement with the predictions of spin-wave theory as applied to the spinel lattice. A precise cancellation of two $T^{5/2}$ terms arising, respectively, from the k^4 terms in the acoustic mode dispersion relation and the k-dependent transformation coefficients to diagonal spin-wave variables gives detailed information on $\omega(k)$ as well as a sensitive test of ferrimagnetic spin-wave theory. The effect on the nuclear resonance of very small anisotropy in the ferromagnetic system is discussed. In the event of a near crossover of the unperturbed nuclear and ferromagnetic uniform precession frequencies, the NMR line is shifted toward lower frequencies. This shift and the accompanying broadening are compared with the experimental observations in the vicinity of 250°K where such a crossover is expected.

I. INTRODUCTION

THE magnetic properties of the ferrimagnetic insulator, $MnFe_2O_4$, have been the subject of considerable study. In particular, the neutron diffraction work of Hastings and Corliss[1] has demonstrated that manganese ferrite has the spinel crystal structure with 80% of the Mn^{2+} ions on the A sites (tetrahedral symmetry) of this lattice. We present here a detailed study of the nuclear magnetic resonance of the Mn^{55} nuclei in this system.

In zero external magnetic field and at a site of tetrahedral symmetry the total Hamiltonian for the nuclei of an S-state ion in a ferrimagnet is given by

$$\mathcal{H}=A\mathbf{I}\cdot\mathbf{S}=AI_zS_z+\tfrac{1}{2}A(I^+S^-+I^-S^+),$$

where A is the hyperfine coupling constant; and I and S are the nuclear and electronic spins. As a result of the strong exchange interactions within the electronic system, and the ferromagnetic anisotropy energy, it is clear that to first order we may neglect the off-diagonal terms and rewrite

$$\mathcal{H}=AI_z\langle S_z\rangle+A\{I_zS_z-\langle S_z\rangle\},$$

where $\langle S_z\rangle$ is the expectation value of the electron spin. Since the electronic ferrimagnetism is the result of this strong exchange interaction any fluctuation in S_z about its expectation value will be predominantly near the exchange frequency ($\sim 10^{12}$) and hence will average to zero over a nuclear precession period. Thus, to first order, in an ordered magnetic medium the hyperfine interaction causes a simple Zeeman splitting of the nuclear energy levels by an amount

$$\Delta E=\hbar\omega_N=|A\langle S_z\rangle|, \quad (1)$$

and one can expect to observe nuclear magnetic resonance at the above frequency. This result is modified somewhat by carrying the calculation through the second order as determined by deGennes *et al.*[2] The result, for a ferromagnetic system, may be written

$$\omega=\omega_N[1-\eta(m_0/M_0)], \quad (2)$$

where η is enhancement factor[3] for the rf field at the nucleus resulting from the indirect excitation of the nuclear resonance in a ferromagnet, and m_0/M_0 is the ratio of the nuclear magnetization to the electronic magnetization. For a single-domain ferromagnetic sample magnetized by an external field H_0 along its easy axis,

$$\eta=H_N/(H_0+H_A),$$

where $H_N=A\langle S_z\rangle/g_N\mu_N$ is the hyperfine field experienced by the nuclei with $g_N\mu_N$ equal to the nuclear g-value times the nuclear magneton; and H_A is the effective ferromagnetic anisotropy field. In a multidomain sample the same expression for ω is appropriate to the nuclei within a domain wall except that the enhancement factor is not the same as the single domain case, but is a complicated function of the position within the domain wall,[3] and of the physical parameters of the wall itself. The origin of this frequency pulling phenomenon can be seen by the following argument. The hyperfine interaction is the isotropic scalar product

* Alfred P. Sloan Foundation Fellow.
† Supported by the Advanced Research Projects Agency.
[1] J. M. Hastings and L. M. Corliss, Phys. Rev. **104**, 328 (1956).
[2] P. G. deGennes, P. Pincus, F. Hartman-Boutron, and J. M. Winter, Phys. Rev. **129**, 1105 (1963).
[3] A. C. Gossard and A. M. Portis, Phys. Rev. Letters **3**, 164 (1959). A. M. Portis and A. C. Gossard, J. Appl. Phys. **31**, 205 (1960).

of I and S. If this were the only term in the Hamiltonian, the excitation spectrum would begin at zero frequency instead of ω_N. In the other limit, if an infinitely large anisotropy field acts on the electronic magnetization and holds it rigidly along the z direction, the nuclei simply precess about the hyperfine field and resonate at ω_N. The real case is clearly in between these two limits. Any finite response of the electronic magnetization tends to lower the NMR frequency. This response can be single domain rotation or wall motion. In either case, Eq. (2) above gives the resonant frequency.

We have observed frequency pulling phenomena for the Mn^{55} nuclei in manganese ferrite at low temperatures. Both the nuclei within single domains and those located within domain walls have their resonant frequency pulled downward as a result of this effect.

In the limit of $\eta m_0/M_0 \ll 1$ (e.g., achieved by application of a relatively large magnetic field or by reducing m_0 by saturating the resonance) the NMR frequency is given by

$$\omega_N = |A\langle S_z\rangle/\hbar| \pm \gamma H_0,$$

the sign being determined by whether the Mn^{55} nuclear moments are parallel or antiparallel to the applied magnetic field H_0. Thus, by measuring the resonance frequency and its field dependence at low temperature, one can determine the magnitude and sign of the hyperfine interaction. These parameters are of interest, for the core polarization mechanism for the hyperfine interaction in s-state ions predicts hyperfine fields of the order of magnitude of 5×10^5 Oe for the $3d^5$ s state of Mn^{2+}; and furthermore predicts $A<0$.[4] These predictions have been verified by the present experiments which find, for the Mn^{55} resonance associated with Mn^{2+} ions on A sites in the spinel lattice, a frequency of 587 Mc/sec with a field dependence indicating $A<0$.

Finally, in the limit where Eq. (1) is valid (zero external field and $\eta m_0/M_0 \ll 1$) we note that the resonance frequency is proportional to $\langle S_z\rangle$; i.e., proportional to the expectation value of S_z on the particular ion in question. Since the nuclear resonance frequency measures only the local $\langle S_z\rangle$, the temperature dependence can be used to measure the A-site *sublattice* magnetization in $MnFe_2O_4$.

Although the spin-wave theory of the low-temperature statistical mechanics of ferromagnetism is over thirty years old,[5] it is only recently that experiments have been performed with sufficient accuracy to allow a detailed comparison of the temperature dependence of the magnetization with the predictions of spin-wave theory. In particular, the NMR in[6] $CrBr_3$ and in[7] EuS demonstrated the $T^{3/2}$ and $T^{5/2}$ terms in the low-temperature expansion, for a three-dimensional Heisenberg ferromagnet; the NMR in[8] $CrCl_3$ showed the linear temperature dependence expected for a two-dimensional ferromagnet; and the pyromagnetic data on[9] Ni pointed to spin-wave type behavior in the ferromagnetic metals. Solt[10] has used the splitting between a pair of magnetostatic modes to precisely measure the temperature dependence of the bulk magnetization in ferrimagnetic YIG, and again finds $T^{3/2}$ and $T^{5/2}$ terms in the temperature dependence. We present here a measurement of the temperature dependence of the sublattice magnetization in ferrimagnetic $MnFe_2O_4$.[11] Again the leading term in the deviation from saturation at low temperatures is proportional to $T^{3/2}$ as expected from the fact that the acoustic mode dispersion relation for a ferrimagnet is proportional to k^2 for low k. However, no $T^{5/2}$ term is observed to within the accuracy of the experiment. This absence of a $T^{5/2}$ term is explained within the framework of spin-wave theory and is shown to be the result of a precise cancellation of two $T^{5/2}$ terms; one arising in the usual manner from the k^4 terms in the acoustic mode dispersion relation and the second arising from the k-dependent transformation coefficients taking one from the single-ion spin deviation operators to the diagonal spin-wave variables.

II. EXPERIMENTAL DETAILS AND THE ORIGIN OF THE NMR SIGNALS

Because of the large enhancement factor in low anisotropy manganese ferrite,[12] the Mn^{55} resonance is detected directly by measuring the change in reflected power from a transmission line loaded with approximately ten grams of polycrystalline $MnFe_2O_4$. In order to maximize the signal to noise and flatten the background in the vicinity of the resonance a simple bridge circuit was used as shown in Fig. 1. The output of a sweep frequency generator was fed through an attenuator to a hybrid junction. This junction splits the input power sending one-half down a shorted transmission line containing the sample and the other half down a similar line which included a line stretcher, an attenuator, and a short. The reflected power from each of these two lines is then fed via the hybrid junction into a crystal detector. Both the phase and amplitude of the rf voltage from the dummy line were variable by means of the line stretcher and attenuator. Thus, a reasonably

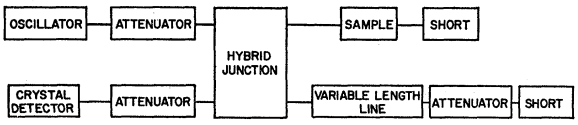

FIG. 1. Schematic diagram of the bridge circuit used to detect the Mn^{55} resonance in $MnFe_2O_4$.

[4] R. E. Watson and A. J. Freeman, Phys. Rev. **123**, 2027 (1961).
[5] F. Block, Z. Physik **61**, 206 (1930).
[6] A. C. Gossard, V. Jaccarino, and J. P. Remeika, Phys. Rev. Letters **7**, 122 (1961).
[7] S. H. Charap, and E. L. Boyd, Phys. Rev. **133**, A811 (1964).
[8] A. Narath, J. Appl. Phys. **35**, 838 (1964).
[9] E. W. Pugh and B. E. Argyle, J. Appl. Phys. **33**, 1178 (1962).
[10] I. H. Solt, J. Appl. Phys. **33**, 1189 (1962).
[11] A. J. Heeger and T. Houston, J. Appl. Phys. **35**, 836 (1964).
[12] W. Palmer, J. Appl. Phys. **33**, 1201 (1962).

good balance could be achieved over a sufficiently broad frequency region to allow easy observation and measurement of the Mn^{55} NMR signal directly on an oscilloscope (see Fig. 5).

NMR signals were observed from Mn^{55} nuclei located both in the bulk of the single domain, and within the domain walls. At the higher temperatures ($T>77°K$) the entire signal was found to arise from nuclei located within the domain walls. This was determined from the fact that the signal diminished rapidly and without shifting in frequency with the application of an applied field; decreasing by more than an order of magnitude in 500 G applied field. The single domain line was apparently too weak to see at this temperature.

In the liquid-helium temperature-range effects from both kinds of indirect excitation were observed. However, the main line (see Fig. 5) at these temperatures originated from nuclei located within the bulk of the single domains. This was again determined from the magnetic field dependence of the signal strength and frequency as shown in Figs. 2 and 3. In Fig. 2 we plot the amplitude of the signal in relative units as a function of the external field H_0. The signal amplitude decreases with increasing field but persists to fields much greater than that needed to magnetize the sample and remove all domain walls. The field dependence of the signal amplitude is the result of the decrease in the enhancement factor with increasing magnetic field. At magnetic fields sufficiently large to saturate the disk-shaped sample ($H_0 \geq 1$ kG) one expects the enhancement factor to be

$$\eta = H_N/(H_0+H_A), \qquad (3)$$

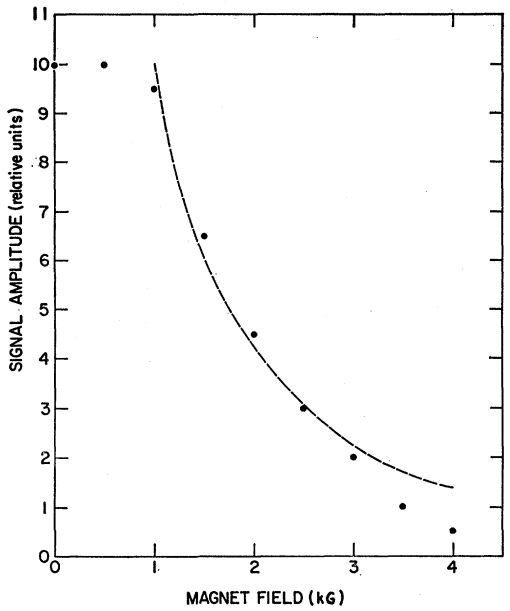

FIG. 2. Magnetic field dependence of the Mn^{55} signal showing the field dependence of the single domain enhancement factor.

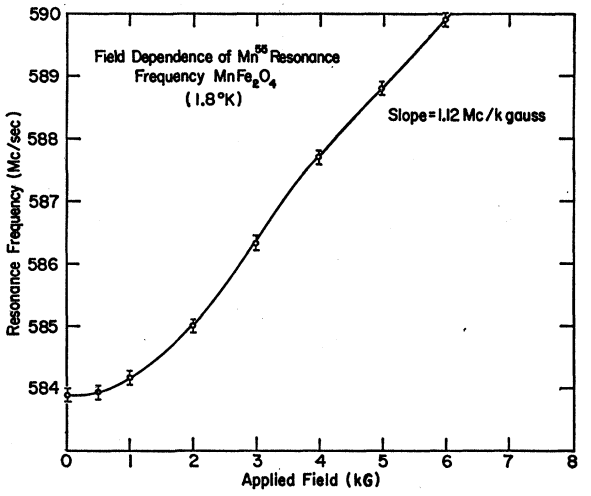

FIG. 3. Magnetic field dependence of the Mn^{55} NMR frequency in ferrimagnetic $MnFe_2O_4$.

where H_N, H_0, and H_A are as defined above. However, for lower fields, when the sample is partially demagnetized the situation is more complex for the internal field is determined not only by the domain in which the nucleus in question is found; but by all the other domains in the sample. For fields where Eq. (3) is valid, one expects the signal to be proportional to η^2; one factor of η for the nuclear magnetization, and one factor for the rf field which couples to this nuclear magnetization. Thus, for fields greater than approximately 1 kG, one expects the signal to be proportional to $1/(H_0+H_A)^2$. The dashed curve of Fig. 2 shows this field dependence with a value for $H_A=800$ G. The fit is satisfactory in the region of applicability. For fields less than about 1 kG, Eq. (3) does not apply for the sample is only partially magnetized. Under these conditions both domain rotation and wall motion will occur, and one cannot calculate the fraction of the magnetic response that is due to domain rotation (i.e., single domain enhancement) in a simple way without making strong assumptions on the mobility of the domain walls.

The field dependence of the resonance frequency is shown in Fig. 3. Note that the resonance frequency *increases* linearly with magnetic field in the saturated sample indicating that the nuclear magnetization is parallel to the applied field. The neutron diffraction data[1] show that $MnFe_2O_4$ is, to first approximation, a two-sublattice ferrimagnet with approximately 5 Bohr magnetons per lattice site. However, since there are twice as many B sites as A sites, the net magnetization is parallel to the iron sublattice or antiparallel to the manganese sublattice as shown schematically in Fig. 4. Consequently, the field dependence of Fig. 3 indicates that Mn^{55} nuclear magnetization is antiparallel to the Mn sublattice magnetization; or I and S are parallel. In order that this be the ground state of the Hamiltonian for the hyperfine interaction, the coupling constant, A,

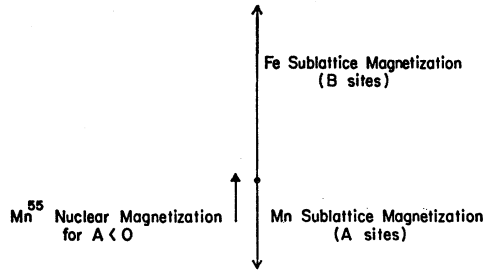

FIG. 4. Schematic diagram of the sublattice structure of $MnFe_2O_4$. The Mn^{55} nuclear magnetization is parallel to the bulk magnetization if $A<0$.

must be negative; i.e., $A<0$. This is in agreement with the core polarization mechanism as discussed in Sec. I.

III. FREQUENCY PULLING PHENOMENA AT LOW TEMPERATURES

The arguments of Sec. II indicate that the main resonance line observed at low temperatures originated from nuclei located within the bulk of the domains; even in the demagnetized sample. However, it is well known that the enhancement factor for wall excitation is typically an order of magnitude larger than that for domain rotation. This is certainly the case even in $MnFe_2O_4$ for temperatures $T>77°K$. This apparent paradox is resolved by noting two essential differences between the enhancement due to wall motion, η_W; and that due to domain rotation η_B

(i) $$\eta_W \gg \eta_B ,$$

(ii) $$\eta_W=\eta_W(x); \quad \eta_B=H_N/(H_0+H_A) ,$$

where x is the coordinate locating the position within the wall. Recalling that the resonance frequency is pulled by an amount [Eq. (2)]

$$\delta\omega=\omega_N\eta(m_0/M_0) ,$$

one concludes that the single domain line will shift a small amount without distorting as a result of the *single-valued* nature of η_B. The wall line, however, will be shifted considerably farther, and will distort and broaden by an amount comparable with the shift. It is this large additional broadening which prevents the wall resonance from being seen at low temperatures where the nuclear magnetization m_0 is large. This is demonstrated nicely by investigating the effect of increasing rf power on the resonance spectrum as shown in Fig. 5. At very low rf powers the entire nuclear spin system has a temperature equal to that of the lattice and we see a single line originating from nuclei within the bulk of the domains. This line is pulled downward by about 3.3 Mc/sec at 1.8°K. Under these conditions the wall line is pulled downward considerably farther and broadened as explained above; and the spectrum is as shown in Fig. 5(a). As the rf power is increased the wall nuclei begin to saturate first since $\eta_W \gg \eta_B$. When this occurs the wall line shifts toward higher frequencies, narrows somewhat, and shows up as an additional absorption on the low-frequency side of the main line [Fig. 5(b)]. At still higher powers [Fig. 5(c)] the wall nuclei are farther into saturation. Those nuclei in the walls with maximum enhancement are by now completely saturated and their frequency is at the unpulled value as shown by the small extra line on the high-frequency side of Fig. 5(c). The main line is, however, still distorted with extra absorption on the low-frequency side. This demonstrates nicely the fact that $\eta_W=\eta_W(x)$, for some of the wall nuclei are fully saturated, while others are only partially so in Fig. 5(c). Finally, at the highest powers available [Fig. 5(d)], the spectrum consists of two essentially symmetric and well-defined resonance lines; one from the bulk nuclei and one from the wall nuclei. The single domain line resonance frequency is independent of power for all of Fig. 5. Note that the final splitting of Fig. 5(d) is 3.3 Mc/sec between the pulled single domain line and the unpulled wall line. This gives an experimental value of

$$f_N\eta(m_0/M_0)|_{\text{exp}}=3.3 \text{ Mc/sec} ,$$

at 1.8°K. Using values of $f_N=584$ Mc/sec, $\eta=H_N/H_A$ with $H_N=556$ kG and $H_A=800$ Oe, one estimates a value of 3.3 Mc/sec for this quantity. It must be emphasized that this power dependence can be used to investigate the pulling only because of the large difference in the two enhancement factors, and because of the pulling itself which places the two resonances at differ-

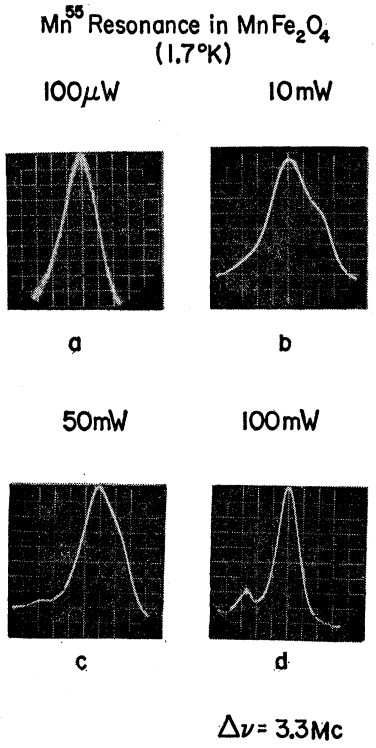

FIG. 5. The effect of increasing rf power on the Mn^{55} resonance spectrum showing the frequency pulling phenomenon.

ent frequencies and thereby inhibits energy diffusion via the strong spin-spin interactions in a ferromagnet.[13] A similar measurement at 4.2°K gives an experimental value of $\Delta f = 1.6$ Mc/sec as compared with an expected $\Delta f = 1.4$ Mc/sec assuming that all quantities other than m_0 are independent of temperature. The 10% discrepancy may reflect the fact that the anisotropy constants K_1 and K_2 are actually very temperature-dependent in this region of temperature.[14]

IV. TEMPERATURE DEPENDENCE OF THE SUBLATTICE MAGNETIZATION

By utilizing the highest powers available at all temperatures it is possible, using the unshifted line of Fig. 5(d), to measure the temperature dependence of the frequency of the unpulled resonance line, and thereby to measure the temperature dependence of the A-site sublattice magnetization. Because of the low anisotropy and large exchange in $MnFe_2O_4$, no significant difference between the magnetization within a wall and that within the bulk is expected.[15] The temperature region of primary interest here is $T < 200$°K. For these temperatures one expects spin-wave theory to apply so that a meaningful comparison of theory and experiment can be made. Furthermore, since manganese ferrite has a relatively high Debye temperature, $\theta_D \sim 600$°K, thermal expansion effects below 200°K should be small, and therefore cannot cause a significantly large implicit temperature dependence of the hyperfine coupling constant A. However, Walsh[16] has shown from paramagnetic resonance studies that the hyperfine coupling constant is intrinsically temperature-dependent varying approximately as

$$A = A(0)[1 - 10^{-6} T^{3/2}].$$

To lowest order, this will simply increase the coefficient of the $T^{3/2}$ term in $M(T)$ and thereby introduce a few percent error in the resulting value for the exchange integral, J_{AB}.

In Fig. 6 we show the Mn^{55} resonance frequency plotted as a function of $T^{3/2}$ where T is the temperature in degrees Kelvin. It is apparent from the straight line character of ν versus $T^{3/2}$ that the initial deviation from saturation at low temperatures is proportional to $T^{3/2}$. The numerical value of the coefficient of the $T^{3/2}$ term is determined by experiment as

$$\nu = \nu_0(1 - 1.2 \times 10^{-5} T^{3/2} + \cdots).$$

There is no $T^{5/2}$ term to within the accuracy of the experiment, although a very small $T^{5/2}$ contribution cannot be ruled out. For temperatures above 160°K, significant deviations from the $T^{3/2}$ line are seen. At

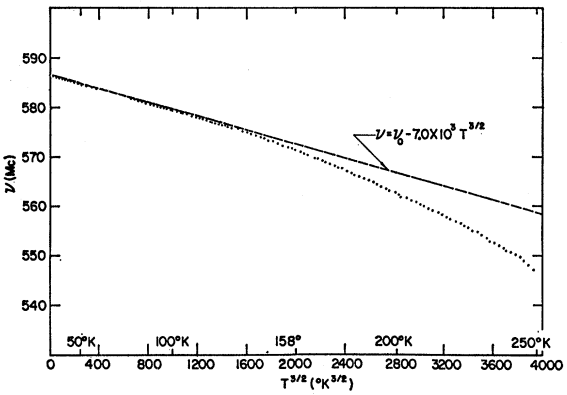

FIG. 6. Temperature dependence of the Mn^{55} resonance frequency and A-site sublattice magnetization in $MnFe_2O_4$.

about 200°K the signal begins to weaken. This loss of signal continues to the point where the line can no longer be seen at temperatures greater than 260°K. This very rapid loss of signal is evidently the result of an increased line width although an attempt to quantitatively measure this broadening was not successful. Linewidth measurements are difficult in this temperature range where the signal is weak and superposed on a large standing wave pattern. The wings of the line become obscured, and the measurement is not meaningful. This additional temperature dependence and broadening will be discussed in detail after developing the theory for the temperature dependence of the sublattice magnetization.

V. THEORY OF THE TEMPERATURE DEPENDENCE AND COMPARISON WITH EXPERIMENT

A detailed spin-wave theory for the ferrimagnetic spinels has been developed by Kaplan.[17] He includes all the details of the lattice structure of the spinel lattice and derives the appropriate dispersion curves for a six sublattice spin-wave theory above a ferrimagnetic ground state. However, it is well known that the fine details of the lattice structure do not affect the k^2 term in the dispersion relation; but come in first in order k^4. This is made clear by comparing the results of a continuum model[18] with those mentioned above. In general, we expect a two sublattice approximation to be exact to order k^2 in all quantities. Therefore, because the physical results are far more apparent within the approximation, we shall employ a two sublattice model. Finally, we shall use the *exact* k^4 term[17] in the acoustic mode dispersion relation in the calculation of $M(T)$.

The interatomic exchange interaction has the form

$$\mathcal{H} = J_{AB} \sum_{j,\delta} S_j \cdot S_{j+\delta}, \qquad (4)$$

where j labels the A sites within the lattice; and δ indi-

[13] H. Suhl, J. Phys. Radium **20**, 333 (1959).
[14] T. G. Blocker, S. K. Ghosh, and A. J. Heeger (to be published).
[15] J. M. Winter, Phys. Rev. **129**, 452 (1961).
[16] W. M. Walsh (private communication).
[17] T. Kaplan, Phys. Rev. **109**, 782 (1958).
[18] H. Kaplan, Phys. Rev. **86**, 121 (1952).

cates the nearest neighbors of an A site. J_{AB} is the exchange integral between ions on the A and B sites. We introduce the boson operators a_j, b_l with the Holstein-Primakoff transformation

$$\begin{aligned} S^+{}_{Aj} &= (2S_A)^{1/2}[1-(a_j{}^+a_j/2S_A)]^{1/2}a_j, \\ S^-{}_{Aj} &= (2S_A)^{1/2}a_j{}^+[1-(a_j{}^+a_j/2S_A)]^{1/2}, \\ S^+{}_{Bl} &= (2S_B)^{1/2}b_l{}^+[1-(b_l{}^+b_l/2S_B)]^{1/2}, \\ S^-{}_{Bl} &= (2S_B)^{1/2}[1-(b_l{}^+b_l/2S_B)]^{1/2}b_l, \\ S^z{}_{Aj} &= S_A-a_j{}^+a_j, \quad S^z{}_{Bl}=-S_B+b_l{}^+b_l. \end{aligned} \tag{5}$$

The individual sublattice spin-wave variables are

$$\begin{aligned} a_k &= \frac{1}{(N_A)^{1/2}}\sum_j e^{i\mathbf{k}\cdot\mathbf{R}_j{}^A}a_j, \\ a_k{}^+ &= \frac{1}{(N_A)^{1/2}}\sum_j e^{-i\mathbf{k}\cdot\mathbf{R}_j{}^A}a_j{}^+, \\ b_k &= \frac{1}{(N_B)^{1/2}}\sum_l e^{-i\mathbf{k}\cdot\mathbf{R}_l{}^B}b_l, \\ b_k{}^+ &= \frac{1}{(N_B)^{1/2}}\sum_l e^{i\mathbf{k}\cdot\mathbf{R}_l{}^B}b_l{}^+. \end{aligned} \tag{6}$$

Substituting these into the exchange Hamiltonian, one obtains to terms second order in creation and destruction operators

$$\begin{aligned} \mathcal{H} = &-J_{AB}Z_AN_AS_AS_B+J_{AB}S_AZ_A\sum_k b_k{}^+b_k+J_{AB}S_BZ_A \\ &\times\sum_k a_k{}^+a_k+J_{AB}N_AZ_A(S_AS_B/N_AN_B)^{1/2} \\ &\times\sum_k \gamma_k(a_kb_k+a_k{}^+b_k{}^+), \end{aligned}$$

where

$$\gamma_k=(1/Z_A)\sum_\delta e^{i\mathbf{k}\cdot\delta},$$

and Z_A is the number of nearest neighbors for an A-site ion. We wish to diagonalize $\mathcal{H}$ and transform to new operators α^+, α, β^+, β such that $(\alpha_k,\alpha_{k'}{}^+)=\delta_{kk'}$, $(\alpha_k,\beta_{k'})=0$, $(\beta_k,\beta_{k'}{}^+)=\delta_{kk'}$. The appropriate transformation is

$$\begin{aligned} a_k &= \alpha_k\cosh\theta_k+\beta_k{}^+\sinh\theta_k, \\ a_k{}^+ &= \alpha_k{}^+\cosh\theta_k+\beta_k\sinh\theta_k, \\ b_k &= \alpha_k{}^+\sinh\theta_k+\beta_k\cosh\theta_k, \\ b_k{}^+ &= \alpha_k\sinh\theta_k+\beta_k{}^+\cosh\theta_k, \end{aligned} \tag{7}$$

where

$$\tanh2\theta_k=-2[(N_AN_BS_AS_B)^{1/2}/(N_AS_A+N_BS_B)]\gamma_k. \tag{8}$$

This removes all nondiagonal terms giving, after substitution,

$$\begin{aligned} \mathcal{H} = &-J_{AB}Z_AN_AS_AS_B-\tfrac{1}{2}J_{AB}Z_A(S_AN_A+S_BN_B) \\ &+\frac{J_{AB}Z_A}{N_B}\sum_k[S_AN_A\sinh^2\theta_k+S_BN_B\cosh^2\theta_k \\ &+(S_AS_BN_AN_B)^{1/2}\gamma_k\sinh2\theta_k](\alpha_k{}^+\alpha_k+1) \\ &+\frac{J_{AB}Z_A}{N_B}\sum_k[S_AN_A\cosh^2\theta_k+S_BN_B\sinh^2\theta_k \\ &+S_AS_BN_AN_B)^{1/2}\gamma_k\sinh2\theta_k](\beta_k{}^+\beta_k+1). \end{aligned} \tag{9}$$

One therefore obtains two branches; an acoustic mode with frequency

$$\omega_k{}^{(1)}\simeq\tfrac{11}{16}J_{AB}\frac{N_AS_AS_B}{N_BS_B-N_AS_A}a^2k^2+\cdots, \tag{10}$$

where a is the lattice constant; and an optical mode

$$\begin{aligned} \omega_k{}^{(2)}\simeq &\frac{J_{AB}Z_A}{N_B}(S_BN_B-S_AN_A) \\ &+\tfrac{11}{16}J_{AB}\frac{N_AS_AS_B}{N_BS_B-N_AS_A}a^2k^2+\cdots. \end{aligned} \tag{11}$$

These are correct to order k^2. However, the k^4 terms are very sensitive to the lattice structure and must be obtained from Kaplan's six sublattice theory. Using $N_B=2N_A$ and $S_B=S_A=S$ the acoustic mode dispersion relation *exact* to order k^4 is given by[17]

$$\begin{aligned} \omega_k{}^{(1)} = &(11/16)J_{AB}Sa^2k^2+E_1k^4 \\ &+E_2[k_x{}^2k_y{}^2+k_x{}^2k_z{}^2+k_y{}^2k_z{}^2], \end{aligned} \tag{12}$$

where

$$E_1=-12J_{AB}S\left[9\left(\frac{11}{12}\right)^2+\frac{83}{144}\right]\frac{a^4}{2^{10}}, \quad E_2=-J_{AB}S\frac{a^4}{2^{10}}.$$

Having obtained the above dispersion relations and defined the transformation we write the temperature dependence of the magnetization as

$$M_A(T)=M_A(0)-g\mu_B\sum_i\sum_k n_k{}^{(i)}(U_i(k))^2, \tag{13}$$

where μ_B is the Bohr magneton $n_k{}^{(i)}$ are the number of thermal spin waves with wave number k in the ith branch, and $U_i(k)$ are the k-dependent transformation coefficients from single sublattice spin deviation operators to the diagonal spin-wave variables. We shall confine the sum (13) to the two modes given above. The effect of the higher order optical modes[17] will be discussed briefly at the end of this section.

Because the spin waves are bosons

$$\begin{aligned} n_k{}^{(1)} &= \langle\alpha_k{}^+\alpha_k\rangle=[\exp\beta E_k{}^{(1)}-1]^{-1}, \\ n_k{}^{(2)} &= \langle\beta_k{}^+\beta_k\rangle=[\exp\beta E_k{}^{(2)}-1]^{-1}, \end{aligned} \tag{14}$$

with $\beta=1/kT$. The transformation coefficients are obtained from Eq. (7)

$$(U_1(k))^2=\sinh^2\theta_k\simeq 1-(11/32)a^2k^2,$$
$$(U_2(k))^2=\cosh^2\theta_k\simeq 2-(11/32)a^2k^2, \quad (15)$$

and are correct to second order in k. Finally, then, the three terms of lowest order are

$$\frac{\Delta M_A}{M_A(0)}=\frac{1}{N_AS_A}\sum_k n_k^{(1)}-\frac{11}{32}\frac{a^2}{N_AS_A}\sum_k k^2n_k^{(1)}+\frac{2}{N_AS_A}\sum_k n_k^{(2)}. \quad (16)$$

The first sum is the usual spin-wave contribution from the acoustic branch and gives rise to terms of $T^{3/2}$, $T^{5/2}$, etc., in the temperature dependence of the sublattice magnetization. The second sum comes from the k-dependent transformation coefficients and gives a $T^{5/2}$ term in lowest order. These two $T^{5/2}$ terms are of opposite sign and tend to cancel one another. Using the dispersion relation (12), this cancellation is nearly exact as shown below and explains the absence of a $T^{5/2}$ term in the experimentally observed temperature dependence. The above sums are evaluated in Appendix A, giving t ıe result

$$\Delta M_A/M_A(0)=AT^{3/2}+(B_1-B_2)T^{5/2}+CT^{3/2}e^{-E_0/\kappa T}, \quad (17)$$

where

$$A=\frac{1}{64\pi^{3/2}S}\left(\frac{k_B}{(11/16)J_{AB}S}\right)^{3/2}\zeta(\tfrac{3}{2}),$$
$$B_1=\frac{11}{(32)^2\pi^{3/2}S}\left(\frac{k_B}{(11/16)J_{AB}S}\right)^{5/2}\tfrac{3}{4}(1.01)\zeta(\tfrac{5}{2}),$$
$$B_2=\frac{11}{(32)^2\pi^{3/2}S}\left(\frac{k_B}{(11/16)J_{AB}S}\right)^{5/2}\tfrac{3}{4}\zeta(\tfrac{5}{2}), \quad (18)$$
$$C=\frac{1}{32\pi^{3/2}S}\left(\frac{k_B}{(11/16)J_{AB}S}\right)^{3/2}, \quad E_0=\tfrac{1}{2}J_{AB}Z_AS,$$

where $\zeta(x)$ is the Reiman zeta function and takes values

$$\zeta(\tfrac{3}{2})=2.61, \quad \zeta(\tfrac{5}{2})=1.34.$$

The final term of Eq. (17) comes from the third sum of (16) and is the contribution from optical-mode spin waves.

TABLE I. Comparison of numerical results of one-parameter spin-wave theory with experiment.

$\Delta\nu=\nu_0-7.0\times10^3T^{3/2}-4.8\times10^{-1}T^{5/2}-5.4\times10^3T^{3/2}e^{-344/T}$

T	$T^{3/2}$	δ_1	δ_2	δ_3	$\Sigma\delta$	ν	ν_{exp}
20	89.5	0.63	···	···	0.63	586.1	586.1
72	600	4.2	···	···	4.2	582.5	582.5
86	800	5.6	···	0.1	5.7	581.0	581.0
100	10^3	7.0	0.05	0.16	7.2	579.5	579.5
113	1200	8.4	0.06	0.3	8.7	578.0	578.0
131	1500	10.5	0.09	0.6	11.2	575.5	575.6
148	1800	12.6	0.13	0.9	13.6	573.1	573.1
158	2000	14.0	0.15	1.2	15.35	571.4	571.4
172	2250	15.75	0.19	1.7	17.6	569.0	568.6
184	2500	17.5	0.22	2.0	19.7	567.0	566.2
200	2820	19.7	0.27	2.7	22.7	564.0	562.7
208	3000	21.0	0.3	3.1	24.4	562.3	560.6
219	3250	22.8	0.34	3.7	26.8	559.9	557.5
230	3500	24.5	0.4	4.2	29.1	557.6	554.3
240	3720	26.0	0.45	4.8	31.3	555.4	550.9
250	3960	27.8	0.5	5.4	33.7	553.0	546.7

It must be emphasized, however, that this precise cancellation of $T^{5/2}$ terms does not occur in a strict two-sublattice approximation. We have employed the two-sublattice model above only to clearly demonstrate the origin of the multiple spin-wave branches and the k-dependent transformation coefficients, but have used the exact acoustic mode dispersion relation as derived by Kaplan. Thus, the absence of the $T^{5/2}$ term provides detailed information on the acoustic mode dispersion relation as well as a sensitive test of ferrimagnetic spin-wave theory.

We note from (17) that as a result of the $T^{5/2}$ cancellation for any value of the exchange integral, J_{AB}, we may use the initial slope of ν versus $T^{3/2}$ in Fig. 6 to determine the coefficient of the $T^{3/2}$ term; and from this slope a value for the exchange integral. Thus,

$$\frac{1}{64\pi^{3/2}S}\left(\frac{k_B}{(11/16)J_{AB}S}\right)^{3/2}\zeta(\tfrac{3}{2})=1.2\times10^{-5},$$
$$\left(\frac{k_B}{(11/16)J_{AB}S}\right)^{3/2}=4.1\times10^{-3},$$

and

$$J_{AB}/k_B\cong 22.7^\circ\text{K}.$$

Having thus determined J_{AB}, there are no adjustable parameters remaining in Eq. (17). Substituting this value for J_{AB}, one obtains the following temperature dependence with a *one-parameter theory*

$$\nu=\nu_0-7.0\times10^3T^{3/2}-4.8\times10^{-1}T^{5/2}-5.4\times10^3T^{3/2}e^{-344/T}+\cdots,$$
$$=\nu_0-\quad\delta_1\quad-\quad\delta_2\quad-\quad\delta_3\quad+\cdots.$$

In Table I we give a numerical compilation of the individual contributions of terms for various temperatures, the sum of these contributions, the resulting calculated frequency, and finally, the observed frequency. One sees that the above one parameter theory gives an excellent fit for temperatures up to 160°K. For higher tempera-

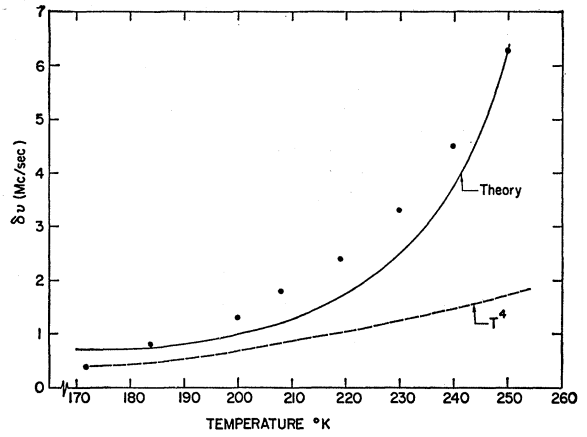

FIG. 7. The discrepancy between the one-parameter spin-wave theory given in the text and the observed temperature dependence of the Mn^{55} NMR frequency. The solid curve is a plot of the theory based on the near crossover of the nuclear and ferromagnetic uniform precession frequencies.

tures the experimental frequency is lower, indicating the importance of higher order terms. In Fig. 7 we show the discrepancy between the one-parameter theory given above including the three lowest order terms of Eq. (17) and the observed frequency. The linear plot emphasizes the strong temperature dependence. For reference, a T^4 dependence is shown as the dashed curve of Fig. 7. One therefore finds that above 160°K, where the lowest terms of Eq. (17) are insufficient, the deviation varies more rapidly than $T^{7/2}$ or even T^4 which are expected to be the next order terms in the spin-wave expansion.

The T^4 term arises in ferrimagnetic spin-wave theory[19] from spin-wave interactions within the acoustic branch. An estimate of the magnitude of the coefficient indicates that the T^4 term should give an insignificant contribution even at the highest temperatures investigated.

Charap[7] has pointed out that the power series expansion into $T^{3/2}$, $T^{5/2}$, $T^{7/2}$, etc., terms is, in reality, only an approximate result when the Brillouin zone boundaries are included. Such a power-series expansion is only valid at temperatures sufficiently low that there is no appreciable excitation near the zone boundary. But in this limit, terms of order $T^{7/2}$ are not important. We shall not consider the $T^{7/2}$ term in any detail for the observed higher order terms vary more rapidly with temperature.

There are several possibilities for explaining the very strong temperature dependence of Fig. 7. The first is a simple thermal expansion of the crystal and a resulting change in the hyperfine constant. However, the temperature dependence seems too strong and the effect too large.[20] A second possibility arises from the fact that $MnFe_2O_4$ is not a perfect normal spinel; but has only 80% of the Mn^{2+} on A sites. This residual disorder will perturb the high-k spin waves and thereby change the temperature dependence. Such a mechanism will be important at high temperature and in fact cannot be ruled out. However, since the exchange energy enters proportional to k^2, one expects the disorder to show up first in terms of order $T^{5/2}$ in the temperature. Such terms are evidently small in view of the excellent agreement obtained above with a uniform spin-wave theory neglecting this disorder. Thus, it appears that the disorder effect is small in nearly stoichiometric $MnFe_2O_4$ although it is important in the more random compositions $Mn_xFe_{3-x}O_4$ for $x<1$.[21]

A third possibility is the excitation of spin waves in the higher order optical modes found by Kaplan.[17] Such excitations would give strongly temperature-dependent terms for the energy gaps are E_0 and $2E_0$, respectively [see Eq. (18)]. Since these modes represent the inequivalence of the two types of A sites, such excitations should broaden the NMR line and if large enough split it into two narrow lines of roughly half the original intensity. This is not in agreement with experiment. A detailed calculation of the effect of these higher order optical modes is complicated by the need to restrict the integration to within the first Brillouin zone and will not be given here.

A final possibility is the existance of bound states for spin waves as predicted by Wortis.[22] Such bound states would make it easier to excite two spin deviations bound as a pair than two spin waves separately. Consequently, the temperature dependence of the magnetization would be more rapid than predicted by simple spin-wave theory as observed in the present experiment. However, one cannot explain the accompanying line broadening with this mechanism; nor are the numbers reasonable. Wortis has argued that the effect of such bound states on the low-temperature thermodynamics would be in proportion to $e^{-\Delta/\kappa T}$ where Δ is the energy of the lowest such bound state. An attempt to fit such a temperature dependence to Fig. 7 yields a value of about 1500°K for Δ or nearly a factor of 3 larger than the Curie temperature. It must be emphasized that all these higher order effects can be considered here only because of the accidental cancellation of the $T^{5/2}$ terms in the spinel lattice.

Although it is not possible to determine uniquely t ıe origin of this discrepancy shown in Fig. 7, we sh ll discuss one possible mechanism in detail; for it can explain not only the curve of Fig. 7, but the loss of signal above 200°K as described in Sec. IV.

VI. COUPLED NUCLEAR-FERROMAGNETIC NORMAL MODES

For temperatures $T>200$°K the ferromagnetic anisotropy energy in $MnFe_2O_4$ is decreasing rapidly toward

[19] F. Keffer and R. Loudon, J. Appl. Phys. **32**, 25 (1961); T. Nakamura and M. Bloch, Phys. Rev. **132**, 2528 (1963).
[20] G. B. Benedek and J. Armstrong, J. Appl. Phys. **32**, 1065 (1961).
[21] H. Callen, A. J. Heeger, D. Hone, and T. W. Houston (to be published).
[22] M. Wortis, Phys. Rev. **132**, 85 (1963).

zero so that the $k=0$ spin-wave frequency approaches the NMR frequency. Under these circumstances, the nuclear resonance is not an exact measure of the magnetization, for these two excitations repel one another as a result of the hyperfine interaction between them. Thus, as the anisotropy and therefore the spin-wave frequencies decrease, the NMR frequency is pushed downward giving an extra temperature dependence over and above that from the temperature dependence of the magnetization. This result comes about because in the region where the two frequencies are comparable, the normal modes for the combined system are not simple spin waves in the electronic system and an isolated precessing nuclear magnetization; but linear combinations of the two. Therefore, as the ferromagnetic anisotropy decreases we expect a shift and a broadening of the nuclear resonance line; the broadening coming from a mixing of some lossy spin-wave character into the nuclear excitation as shown below. The temperature dependence of this additional shift is determined by that of the ferromagnetic anisotropy and is not directly related to $M(T)$.

We consider the simple model of a ferromagnetic sample with magnetization $\mathbf{M}$, coupled to a 100% abundant nuclear species with magnetization $\mathbf{m}$, via the hyperfine interaction. In terms of $\mathbf{M}$ and $\mathbf{m}$ the hyperfine interaction takes the form

$$\mathcal{H}=\alpha\mathbf{m}\cdot\mathbf{M},$$

where $\alpha=(1/N)(A/g_N\mu_N g_e\mu_B)$ and N is the number of spins, g_N and g_e are the nuclear and electronic g values, and μ_N and μ_B are the nuclear and Bohr magnetons. We further assume an effective anisotropy field H_A acting in the z direction. The resulting total field experienced by the electronic spins is

$$\mathbf{H}_e=\alpha m_x\hat{x}+\alpha m_y\hat{y}+(\alpha m_z+H_A)\hat{z},$$

and that seen by the nuclear spins is

$$\mathbf{H}_N=\alpha M_x\hat{x}+\alpha M_y\hat{y}+\alpha M_z\hat{z}.$$

We note that $\alpha<0$ for the s-state ions of the $3d$ transition metals so that the nuclear and electronic magnetizations are antiparallel; $m_z=-m_0$, and $M_z=M_0$. The coupled equations of motion then are

$$dM^+/dt=i|\gamma_e|[M^+(H_A+H_{AN})+m^+H_N]-(M^+/\tau),$$

and

$$dm^+/dt=i\gamma_N[m^+H_N+H_{AN}M^+],$$

where $H_N=-\alpha M_0$ and $H_{AN}=\alpha m_0$ and τ is the phenomenological relaxation time introduced to represent relaxation in the ferromagnetic system. Solving the secular determinant, one finds the following frequencies for the combined modes:

$$2\omega=|\gamma_e|(H_A+H_{AN})+\gamma_N H_N+(i/\tau)\pm\left\{[|\gamma_e|(H_A+H_{AN})-\gamma_N H_N]^2-\frac{1}{\tau^2}-2\gamma_N H_N\frac{i}{\tau}+2|\gamma_e|(H_A+H_{AN})\frac{i}{\tau}\right\}^{1/2}.$$

The real part is given by

$$2\omega_{\text{real}}=(\beta+1)\gamma_N H_N\pm\gamma_N H_N\left\{\left[(\beta-1)^2+\frac{1}{\gamma_N^2H_N^2\tau^2}+4\beta\frac{H_{AN}}{H_A}\right]^2-16\beta\frac{1}{\gamma_N^2H_N^2\tau^2}\frac{H_{AN}}{H_A}\right\}^{1/4},\quad(19)$$

where $\beta=|\gamma_e|H_A/\gamma_N H_N$. Note that for $\beta\gg1$, the two frequencies are

$$\omega_1\cong|\gamma_e|H_A\quad\text{and}\quad\omega_2\cong\gamma_N H_N,$$

as expected for large anisotropy. However, for $\beta\sim1$ the two modes are shifted relative to these values. A value for β consistant with the above model may be obtained from anisotropy measurements on single crystal $MnFe_2O_4$.[12]

The solid curve shown in Fig. 7 is a plot of Eq. (19). A value for τ such that $\gamma_N H_N\tau\cong14$, is determined by fitting Eq. (19) to the single point at 250°K. The fit is quite satisfactory considering the fact that the experiments were done in zero field in a demagnetized sample so that the above model is only approximately applicable. The fit can be made almost exact by choosing slightly different values for H_A and τ. Since the anisotropy in the manganese-iron ferrite system is a strong function of composition[12] such a choice is not unreasonable. However, this is not shown in Fig. 7.

Thus, we conclude that the frequency shifts shown in Fig. 7 and the accompanying broadening of the NMR line can be explained as the result of a near crossover of the uniform precession frequencies of the ferromagnetic and nuclear systems, respectively.

APPENDIX

The temperature dependence of the sublattice magnetization is given by Eq. (16).

$$\frac{\Delta M_A}{M_A(0)}=\frac{1}{N_AS_A}\sum_k n_k^{(1)}-\frac{11}{32}\frac{a^2}{N_AS_A}\sum_k k^2n_k^{(1)}+\frac{2}{N_AS_A}\sum_k n_k^{(2)}+\cdots.$$

We consider these terms one at a time:

$$\sum_k n_k^{(1)}=\sum_k 1/(e^{\beta E_k}-1).$$

Changing from the sum to an integral,

$$\frac{1}{N_A}\sum_k n_k^{(1)}=\frac{V}{(2\pi)^3N_A}\int d^3k[e^{\beta E_k}-1]^{-1}$$
$$=\frac{V}{(2\pi)^3N_A}\sum_{p=1}^{\infty}\int d^3k e^{-p\beta E_k},$$

where

$$E_k=Dk^2+E_1k^4+E_2(k_x^2k_y^2+k_x^2k_z^2+k_y^2k_z^2).$$

Substituting, we find

$$(1/N_A)\sum_k n_k^{(1)}=(V/(2\pi)^3N_A)\sum_{p=1}^{\infty} d^3k e^{-p\beta Dk^2}$$
$$\times[1-p\beta E_1k^4-p\beta E_2(k_x^2k_y^2+k_x^2k_z^2+k_y^2k_z^2)].$$

Now

$$\frac{V}{(2\pi)^3N_A}\sum_{p=1}^{\infty}\int d^3k e^{-p\beta Dk^2}=\frac{V}{2\pi^2N_A}\sum_{p=1}^{\infty}\int k^2e^{-p\beta Dk^2}dk$$
$$=\frac{V}{4\pi^2N_A}\left(\frac{\kappa T}{D}\right)^{3/2}\sum_{p=1}^{\infty}\frac{1}{p^{3/2}}\Gamma(\tfrac{3}{2})$$
$$=\frac{V}{8\pi^{3/2}a^3N_A}\left(\frac{\kappa T}{(11/16)JS}\right)^{3/2}\zeta(\tfrac{3}{2})$$
$$=\frac{1}{64\pi^{3/2}}\left(\frac{\kappa T}{(11/16)JS}\right)^{3/2}\zeta(\tfrac{3}{2}).$$

Similarly,

$$\frac{V}{(2\pi)^3N_A}\sum_{p=1}^{\infty}\frac{pE_1}{\kappa T}\int d^3kk^4e^{-p\beta Dk^2}$$
$$=\frac{V}{2\pi^2N_A}\sum_{p=1}^{\infty}\frac{pE_1}{\kappa T}\int_0^{\infty}k^6e^{-p\beta Dk^2}dk$$
$$=\frac{V}{4\pi^2N_A}\sum_{p=1}^{\infty}\frac{pE_1}{\kappa T}\left(\frac{\kappa T}{D}\right)^{7/2}\int_0^{\infty}x^{5/2}e^{-px}dx$$
$$=\frac{15V}{32\pi^{3/2}N_A}\left(\frac{E_1}{D}\right)\left(\frac{\kappa T}{D}\right)^{5/2}\zeta(\tfrac{5}{2})$$
$$=\frac{11}{(32)^2\pi^{3/2}}\left(\frac{3}{4}\right)(1.009)\left(\frac{\kappa T}{(11/16)JS}\right)^{5/2}\zeta(\tfrac{5}{2}),$$

and

$$\frac{V}{(2\pi)^3N_A}\sum_{p=1}^{\infty}\frac{pE_2}{\kappa T}\int d^3k[k_x^2k_y^2+k_x^2k_z^2+k_y^2k_z^2]e^{-p\beta Dk^2}$$
$$=\frac{3V}{(2\pi)^3N_A}\int dk_z e^{-p\beta Dk_z^2}$$
$$\times\int dk_yk_y^2e^{-p\beta Dk_y^2}\int dk_xk_x^2e^{-p\beta Dk_x^2}$$
$$=\frac{3V}{4(2\pi)^3N_A}[\Gamma(\tfrac{3}{2})]^3\left(\frac{E_2}{D}\right)\left(\frac{\kappa T}{D}\right)^{5/2}\zeta(\tfrac{5}{2})$$
$$=\frac{11}{(32)^2\pi^{3/2}}\frac{3}{4}(0.001)\left(\frac{\kappa T}{(11/16)JS}\right)^{5/2}\zeta(\tfrac{5}{2}).$$

The second sum is

$$-\frac{11}{32}\frac{a^2}{N_A}\sum_k k^2n_k^{(1)}=-\tfrac{11}{32}a^2\frac{V}{2\pi^2N_A}\int_0^{\infty}\frac{k^4dk}{e^{\beta Dk^2}-1}$$
$$=-\frac{11}{(32)^2\pi^{3/2}}\frac{3}{4}\zeta(\tfrac{5}{2})\left(\frac{\kappa T}{(11/16)JS}\right)^{5/2}.$$

Finally, the third sum is

$$\frac{2}{N_A}\sum_k n_k^{(2)}=\frac{2V}{(2\pi)^3N_A}\int d^3k[e^{\beta E_k^{(2)}}-1]^{-1}$$
$$=\frac{2V}{(2\pi)^3N_A}\sum_p\int d^3k e^{-p\beta E_k^{(2)}},$$

where

$$E_k^{(2)}=E_0+Dk^2.$$

Since $E_0/\kappa T>1$ for all temperatures of interest, we keep only the first term.

$$\frac{2}{N_A}\sum_k n_k^{(2)}\cong\frac{2V}{(2\pi)^3N_A}e^{-E_0/\kappa T}\int d^3k e^{-Dk^2/\kappa T}$$
$$=\frac{1}{32\pi^{3/2}}\left(\frac{\kappa T}{(11/16)JS}\right)^{3/2}e^{-E_0/\kappa T}.$$

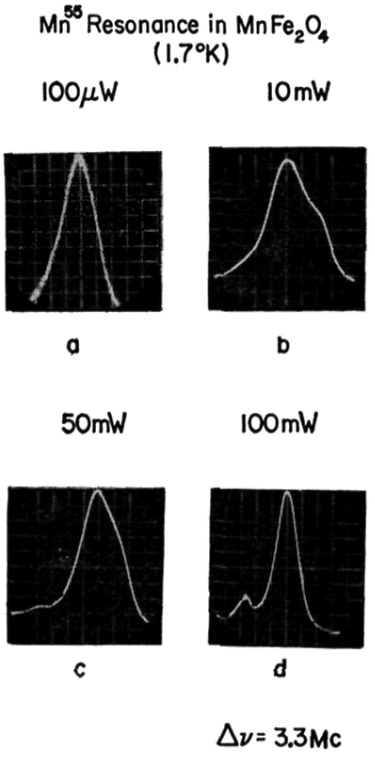

FIG. 5. The effect of increasing rf power on the Mn^{55} resonance spectrum showing the frequency pulling phenomenon.